Journal of Alloys and Compounds 509 (2011) 1830–1835

Contents lists available at ScienceDirect

Journal of Alloys and Compounds

journal homepage: www.elsevier.com/locate/jallcom

Structural and optical characterization of $BaSnO_3$ nanopowder synthesized through a novel combustion technique

A.S. Deepa [a], S. Vidya [a], P.C. Manu [a], Sam Solomon [b], Annamma John [b], J.K. Thomas [a,*]

[a] Electronic Materials Research Laboratory, Department of Physics, Mar Ivanios College, Thiruvananthapuram, Kerala 695 015, India
[b] Department of Physics, St. John's College, Anchal, Kollam District 691306, India

ARTICLE INFO

Article history:
Received 2 September 2010
Received in revised form 3 October 2010
Accepted 12 October 2010
Available online 13 November 2010

Keywords:
Combustion Synthesis
Barium stannate
Nanoparticles
FTIR
Raman
Optical studies

ABSTRACT

Nanocrystalline Barium stannate ($BaSnO_3$) was synthesized through auto-ignited combustion technique. The X-ray diffraction studies of $BaSnO_3$ nanoparticles reveals that the nanopowder is single phase, crystalline, and has a cubic perovskite structure with a lattice constant $a = 4.115$ Å. The average particle size calculated from full width half maximum (FWHM) using Scherer formula is ~25 nm. The phase purity of the powder was further examined using Fourier transform infrared spectroscopy, Raman spectroscopy and transmission electron microscopic techniques. XRD pattern of $BaSnO_3$ was refined for atomic coordinates, lattice parameters and occupancies using Rietveld analysis. Vibrational analysis of sample shows that there is a phase transition from distorted cubic to ideal cubic structure during heat treatment. The thermal stability of $BaSnO_3$ nanopowder has been confirmed using thermo gravimetric analysis (TGA) and differential thermal analysis (DTA). The particle size of the as-prepared powder from transmission electron microscopy was found to be in the range 20–30 nm. The absorption spectra and photoluminescence spectra of the sample were also studied. The band gap determined was 2.887 eV and found to be a semiconductor.

© 2010 Elsevier B.V. All rights reserved.

1. Introduction

Synthesis of advanced functional materials as nanometer sized grains has gained tremendous attention in the recent period. Properties of nanocrystals deviate from those of single crystals and coarse-grained polycrystals due to their reduced size and numerous interfaces between adjacent grains. High surface to volume ratio of nanocrystals lead to enhanced mechanical, electrical, dielectric, magnetic and optical properties.

The double oxides of the general formula, ABO_3, formed between the oxides of alkaline-earth metals (A = Ca, Sr and Ba) and those of some of the group IV elements are of great industrial and technological importance. Barium stannate, $BaSnO_3$, belongs to the family of analogous alkaline-earth stannates ($MSnO_3$ where M = Ca,Sr and Ba) which is an n-type semiconducting material.[1,2]. It has been widely investigated on its dielectric, thermal, and photocatalytic properties as an important ceramic material in pure as well as in doped forms. These stannates have also been studied for their potential applications as sensor materials for host of gases, including CO, HC, H, Cl, NO [3–7]. Recently, Ostrick et al. [8] have reported the results of Hall measurements on $BaSnO_3$ at high temperatures to elucidate the nature of defects prevailing in the material. The band gap of barium stannate was reported to be 3.1 eV, generally desired for gas sensor materials [9]. Additionally, the results by Borse et al. [10] and Yuan et al. [11] suggest that $BaSnO_3$-based systems could be good candidates for photo catalytic applications. Mizoguchi et al. [12] reported that $BaSnO_3$ exhibits strong near-infrared luminescence at room temperature. Suggestions have also been made that, by combining $BaTiO_3$ with $BaSnO_3$ (BTS), multifunctional ceramic sensors which can detect temperature, relative humidity and gases such as prozylene, acetylene and ethylene at the ambient temperatures and pressures can be engineered [13].

Generally conventional solid-state ceramic route was used for the preparation of stannate based compounds. It requires prolonged calcination at about 1200 °C for several hours along with intermediate grinding in order to obtain reasonable phase purity. The coarse-grained powders synthesized using the conventional solid-state route have the disadvantages of larger particle size, high temperature processing and lower phase purity [14]. In the last few years many preparation procedures have been reported to obtain fine-grained $BaSnO_3$ powders at relatively low temperatures. Different hydrothermal methods or sol–gel processes have been developed and reported in literatures [15–20]. Recently, a lyothermal synthesis at 250 °C has been reported by Lu and Schmidt [21]. Various precursor complexes, co-precipitation and polymerised complex methods have also been developed to obtain barium stannate powders [22–25]. Based on the exothermic reaction of suitable solids, self-propagating high temperature syntheses

* Corresponding author. Tel.: +91 471 2530887; fax: +91 471 2532445.
E-mail address: jkthomasemrl@yahoo.com (J.K. Thomas).

0925-8388/$ – see front matter © 2010 Elsevier B.V. All rights reserved.
doi:10.1016/j.jallcom.2010.10.056

are also used to prepare $BaSnO_3$ [26,27]. Most of these method either required high temperature treatment or encountered difficulty in obtaining single phase $BaSnO_3$.

In this paper we report for the first time the optimal conditions to prepare phase pure perovskite semiconducting $BaSnO_3$ by a modified auto-igniting combustion route. The structure, thermal behavior, vibrational spectroscopic and optical studies of the nanopowder is also reported.

2. Experimental

The basic step for the preparation of $BaSnO_3$ by the modified combustion method is to prepare a solution containing ions of Ba and Sn. In the typical synthesis, aqueous solution containing ions of Ba and Sn were prepared by dissolving stoichiometric amount of $Ba(NO_3)_2$(99.99%, CDH, India), and $SnCl_4{\cdot}5H_2O$(99.9% Sigma Aldrich)in double distilled water (200 ml) in a glass beaker. To get the precursor complex, this stoichiometric solution was mixed with citric acid solution, keeping the citric acid to the cation ratio unity. Concentrated HNO_3 was then added to the precursor. The product was stirred well for uniform mixing and a clear solution with no precipitate or sedimentation was obtained. Liquor ammonia was added to the solution to adjust the oxidant fuel ratio to unity. The solution containing the precursor mixture at a pH of ~7.0 was heated using a hot plate at ~250 °C in a ventilated fume hood. The solution boils and undergoes dehydration followed by decomposition leading to a smooth deflation producing foam. On persistent heating the foam gets auto-ignited giving a voluminous fluffy pale yellow powder of $BaSnO_3$ due to self propagating combustion.

In the preparation of samples by combustion process, the earlier workers have used poly vinyl alcohol and urea as the complexing agent and fuel respectively. In such case high temperature annealing of the as-prepared powder was required to get a phase pure $BaSnO_3$ powder [28,29]. But in the present modified combustion method, citric acid was used as the complexing agent instead of poly vinyl alcohol and urea was replaced with ammonia. By this change of complexing agent and oxidant fuel system it was possible to obtain $BaSnO_3$ nanoparticles through the modified combustion process and the usual calcinations for prolonged duration at high temperature is not needed.

Structure of the as-prepared powder was examined by powder X-ray diffraction (XRD) technique using a Bruker D-8 X-ray Diffractometer with Nickel filtered Cu K_α radiation. The differential thermal analysis (DTA) and thermo gravimetric Analyses (TGA) were carried out using Perkin–Elmer TG/DT thermal analyzer in the range 30–1000 °C at a heating rate of 20 °C/min in nitrogen atmosphere. The Infrared (IR) spectra of the samples were recorded in the range 400–4000 cm^{-1} on a Thermo-Nicolet Avatar 370 Fourier transform infrared (FTIR) spectrometer using KBr pellet method. The Fourier transform–Raman spectrum of the nanocrystalline $BaSnO_3$ was carried out at room temperature in the wave number range 50–1200 cm^{-1} using Bruker RFS/100S Spectrometer at a power level of 150 mW and at a resolution of 4 cm^{-1}. The samples were excited with an Nd:YAG laser lasing at 1064 nm and the scattered radiations were detected using Ge detector. Particulate properties of the combustion product were examined using transmission electron microscopy (TEM, Model-Hitachi H-600 Japan) operating at 200 kV. The samples for transmission electron microscope (TEM) were prepared by ultrasonically dispersing the powder in methanol and allowing a drop of this to dry on a carbon-coated copper grid. The photoluminescence spectra of the samples were measured using Flurolog®-3 spectroflurometer. The photons from the source were filtered by an excitation spectrometer. The monochromatic radiation was then allowed to fall on the disc samples and the resulting radiation was filtered by an emission spectrometer and then fed to a photomultiplier detector. The variation of intensity was recorded as a function of wavelength. The absorption spectra were also measured using a Jasco UV–visible spectrophotometer.

3. Results and discussion

The XRD pattern of the as-prepared powder obtained directly after combustion synthesis is shown in Fig. 1a. All the peaks are indexed for cubic structure having the calculated lattice constant as 4.115 Å and it agrees very well with the reported XRD data in the JCPDS file (JCPDS card No. 15-0780), for $BaSnO_3$ which indicate that the formation of $BaSnO_3$ phase was complete during the combustion process itself without a need for a calcination step. The crystalline size calculated from full width half maximum (FWHM) using the Scherrer formula for the major (0 1 1) reflection is found to be ~25 nm. It may be noted that a single phase $BaSnO_3$ material can be obtained through solid-state reaction route only after prolonged calcinations of the reaction mixture at 1200 °C with multiple intermediate grindings [28,29]. In the XRD pattern of as-prepared sample, reflections of very small intensity can also be seen

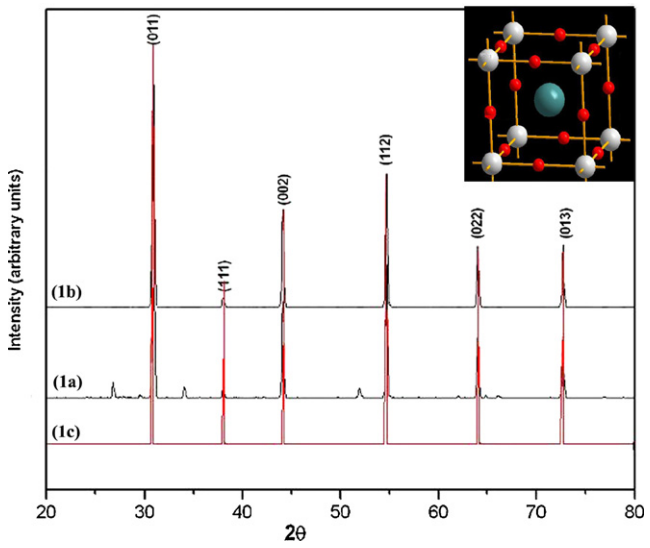

Fig. 1. XRD patterns of (a) as-prepared $BaSnO_3$ (b) $BaSnO_3$ annealed at 1200 °C and (c) powder pattern obtained from Rietveld analysis.

at 34.076° and 54.679°. On examining the JCPDS files it is seen that SnO_2 (71-652) posses peaks at 33.874° and 54.752° and $BaCO_3$ (45-1471) posses peaks at 34.096° and 54.698°. These reflections are likely due to traces of barium carbonate present in the sample. Since the combustion process takes place in very short duration of time these impurities may remain in the as-prepared sample. The XRD of the sample annealed at 1200 °C is shown in the Fig. 1b. It is clear from the XRD pattern that no above mentioned peaks are present. The particle size calculated from the XRD of the annealed sample is about 65 nm.

Based on the Rietveld analysis and SpuDS prediction the structural parameters of $BaSnO_3$ were found to be cubic perovskite structure with space group #221 ($Pm3m$) and lattice parameter 4.109 Å. Fig. 1c shows the powder pattern obtained from the Rietveld analysis. The similarity between the experimental and simulated pattern shows that the as-prepared nanoparticles posses cubic symmetry. The inset figure shows the primitive cubic structure of the $BaSnO_3$ perovskite material. It can be noted that Ba^{2+} ions occupy the cube centre whereas the $Sn^{4+}$and O^{2-} ion are at intermittent edges of the cube. Table 1 summarizes atomic coordinates, lattice parameters and occupancies of $BaSnO_3$.

The thermal characterization of the nanoparticles of $BaSnO_3$ synthesized through the combustion process is carried out using differential thermal analysis (DTA) and thermo gravimetric analysis (TGA) up to 1000 °C at heating rate of 10 °C/min in nitrogen atmosphere. The DTA and TGA curves of the as-prepared $BaSnO_3$ powders obtained directly after combustion is shown in Fig. 2. The TGA curve shows a weight loss of 10% at about 100 °C, which may be due to the expulsion of adsorbed moisture present in the sample.

Table 1
Structural details of $BaSnO_3$.

Atomic co-ordinates of $BaSnO_3$					
Atom	Site	*x*	*y*	*z*	Occ.
Ba	1b	0.5	0.5	0.5	1
Sn	1a	0	0	0	1
O	3d	0	0	0.5	0

Crystal Structure: Cubic.
Space group: $Pm3m$ (#221).
Lattice parameters: $a = b = c = 4.109$ Å, $\alpha = \beta = \gamma = 90°$.
Volume of unit cell = 69.38 $Å^3$.
Theoretical density: 7.277 g/cm^3.

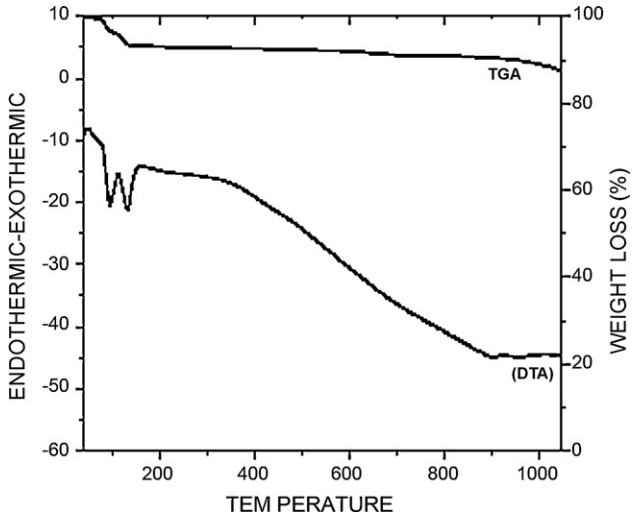

Fig. 2. The DTA and TGA curves of as-prepared $BaSnO_3$ nanoparticles.

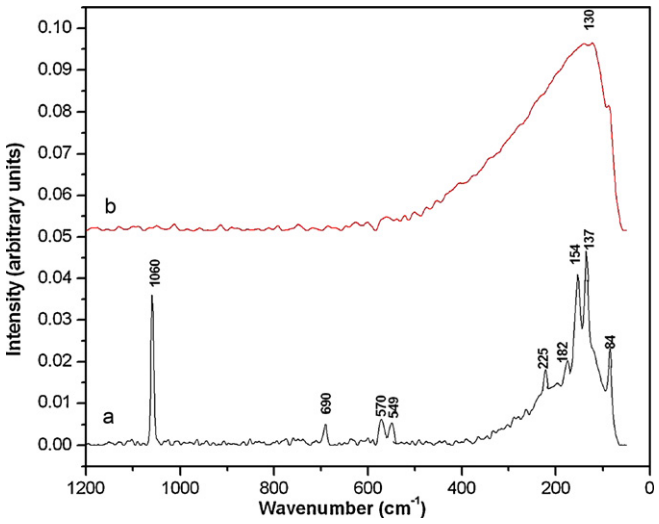

Fig. 3. Raman spectra of $BaSnO_3$ nanoparticles (a) as-prepared (b) heated at 1200 °C.

Thereafter there is a very small weight change of ~2% occurring in the sample around 1000 °C, which may be due to the decomposition of $BaCO_3$ traces present in the sample. No weight loss other than those mentioned above implies that the combustion is complete and no organic matter is present in the sample. The enthalpy changes observed in the DTA curve at different temperatures can be attributed to surface reactions taking place in $BaSnO_3$. There is also no evidence of any phase transition-taking place in the sample up to this temperature.

The nanocrystalline $BaSnO_3$ has cubic structure with space group $Pm3m(O_h)$, with one formular in the unit cell [30,31].The factor group analysis using the standard correlation method [32,33] gives the irreducible representation at $k = 0$ as

$$\Gamma = 3F_{1u}\,(\mathrm{IR}) + F_{2u}\,(\mathrm{silent})$$

The irreducible representation shows that the sample has no Raman active modes and hence does not give a first order Raman spectrum. However, the recorded Raman spectrum shows certain well defined bands. The spectrum obtained for the $BaSnO_3$ powder prepared through the modified combustion method in the present study, is similar to that reported by Cerda et al. [31] where the sample is prepared by the sol–gel method. In order to eliminate the carbonate peaks the sample was heated up to 1200 °C. The observed Raman bands can be assigned on the basis of the modes of vibrations of SnO_6 octahedron, which has O_h symmetry, in the distorted perovskite structure. The six fundamental vibrations of SnO_6 octahedron are the symmetrical stretching mode v_1A_{1g}, asymmetric stretching modes v_2E_g and v_3F_{1u}, asymmetric bending mode v_4F_{1u}, symmetric bending mode v_5F_{2g} and the inactive mode v_6F_{2u}.

Figs. 3 and 4 shows Raman and IR spectra of as-prepared and heated nanocrystalline $BaSnO_3$ respectively. The observed Raman and IR bands, their relative intensities and the band assignments are shown in Table 2.

The three Raman active modes v_1A_{1g}, v_2E_g and v_5f_{2g} are observed as medium or highly intense bands at 690, 570 and 137 cm^{-1}, respectively. The E_g mode is broadened and shows a doublet structure with the other component at 549 cm^{-1}. The IR active v_3F_{1u} mode appears as a very strong absorption band at 629 cm^{-1} in the spectrum. The Raman active v_2E_g mode has become active in the IR spectrum and is observed as a doublet at 568 and 579 cm^{-1}. The splitting of the degenerate modes and the appearance of inactive modes in the spectra suggest a lowering of symmetry due to distortion.

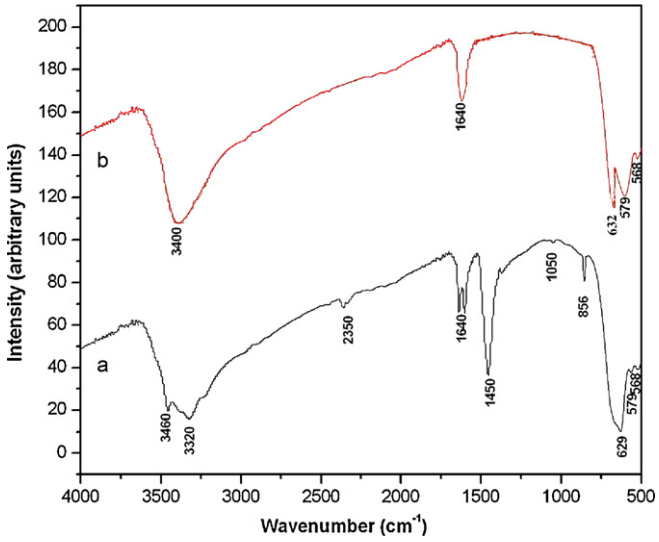

Fig. 4. FTIR spectra of $BaSnO_3$ nanoparticles (a) as-prepared (b) heated at 1200 °C.

The intense sharp peak at 1060 cm^{-1} in the Raman spectrum is due to the presence of $BaCO_3$ in the combustion method product. The IR spectrum also shows the presence of $BaCO_3$ in the sample. The absorption bands at 856, 1050 and 1450 cm^{-1} are the characteristic bands of $BaCO_3$. Thus from the vibrational analysis and the XRD patterns it can be concluded that the trace of the additional phase present in the as-prepared sample is that of $BaCO_3$.

The Raman spectra of heated sample up to 1200 °C shows no first order Raman bands which confirms that on heating the crystal has changed to ideal cubic perovskite. In the IR spectra no bands

Table 2
Band assignments.

Raman	IR	Band assignment
690m		v_1A_{1g}
	629vs	v_3F_{1u}
570w, 549vw	568s, 579vw	v_2E_g
225m		v_4F_{1u}
182m		v_6F_{1u}
154, 137vs		v_5F_{2g}
84s		Lattice mode

vs – very strong; vw – very weak m – medium; w – weak; s – strong.

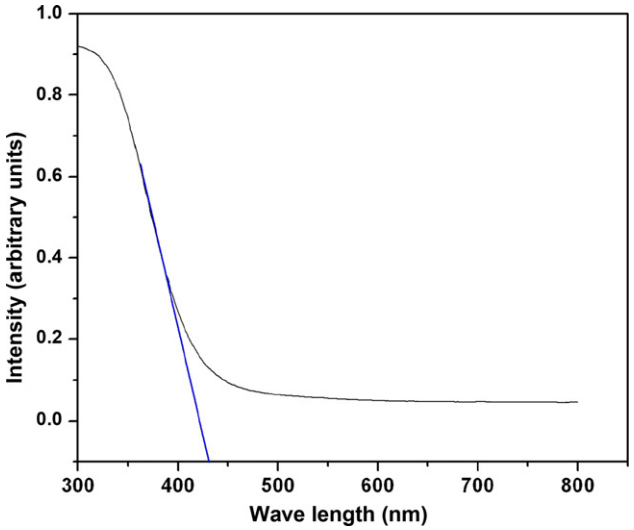

Fig. 5. Absorption spectra $BaSnO_3$ nanopowder obtained through combustion synthesis

corresponding to $BaCO_3$ can be identified. However, in the IR spectrum the F_{1u} mode is observed as a very strong and sharp band at 632 cm^{-1}which indicates that the $BaSnO_3$ which had a distorted cubic structure, on heating at 1200 °C for 4 h, has transformed to an ideal cubic structure. Thus Raman spectroscopy serves as an effective tool to explore the loss of symmetry and formation of defects such as oxygen vacancies and F-centers.

Absorption spectra of the sample measured in the range from 200 to 800 nm is given in the Fig. 5. From the absorption spectra it is clear that sample absorbs heavily within the UV region but moderately in the visible region. The absorption spectrum of $BaSnO_3$ exhibits typical optical behavior of a wide-band gap semiconducting oxide having an intense absorption band around 425 nm with a steep edge. It reveals that $BaSnO_3$ nanomaterials can readily respond to ultraviolet. The optical absorption in the wavelength region shorter than 400 nm is mainly attributed to the electron transition from the top of the valence band to the bottom of the conduction band [34]. Also the reflectance spectrum as shown in the Fig. 6 indicates the maximum reflectance in the visible region which substantiates our interpretation of maximum UV absorption. Such materials found applications in filters and sensors for UV radiation.

There is a small degree of visible attenuation which gives the sample a slight colour cast. When white light passes through or is reflected by a colored substance, a characteristic portion of the mixed wavelengths is absorbed. The remaining light will then assume the complementary color to the wavelength(s) absorbed and the substance will appear to be in that colour. Thus, absorption of 420–430 nm which corresponds to violet region of visible spectra renders the substance a pale yellow colour which is the complementary colour of violet.

A semiconductor is characterized by its electronic band structure. The energy difference between highest occupied molecular orbital (HOMO) and lowest unoccupied molecular orbital (LUMO) is termed as bang gap energy (E_g). The band gap energy is determined by extrapolating the wavelength of the onset absorption in UV region as illustrated in the Fig. 5 and solving the relation $E = hc/\lambda$. The corresponding band-gap for the wavelength 429.669 nm is 2.891 eV.

In semiconductors the absorption coefficient near the fundamental edge depends on photo energy. In high energy absorption region dependence on photon energy is expressed by the Tauc's equation [35]. According to the Tauc relation, the absorption coefficient, a, for direct band gap material is given by

$$\alpha(h\nu) = B(h\nu - E_g)^m$$

where B is an energy independent constant is the absorption coefficient E_g is the optical band gap energy, h is the Planck's constant, ν is the frequency of incident photon and m is an index which depends on the nature of electronic transition responsible for the optical absorption. Values of m for allowed direct and non-direct transitions are 1/2 and 2, respectively.

Optical transitions of $BaSnO_3$ are known to be an indirect one. Fig. 7 shows a Tauc's plot of the optical absorption spectrum measured at room temperature for $BaSnO_3$ nanopowder. The indirect optical energy gap can be obtained from the intercept of the resulting linear region with the energy axis at $(\alpha h\nu)^2 = 0$. Thus determined band gap of $BaSnO_3$ is 2.887 eV which is approximately equal to what we got from the absorption spectra. This experimentally obtained band gap is found to be lower than the standard one [36]. The obtained value is similar as that obtained by Koferstein and Yakuphanoglu [37] which they reported for germanium doped $BaSnO_3$. Such a change in band gap can be partially attributed to the quantum size effects, i.e. increased electronic energy levels when

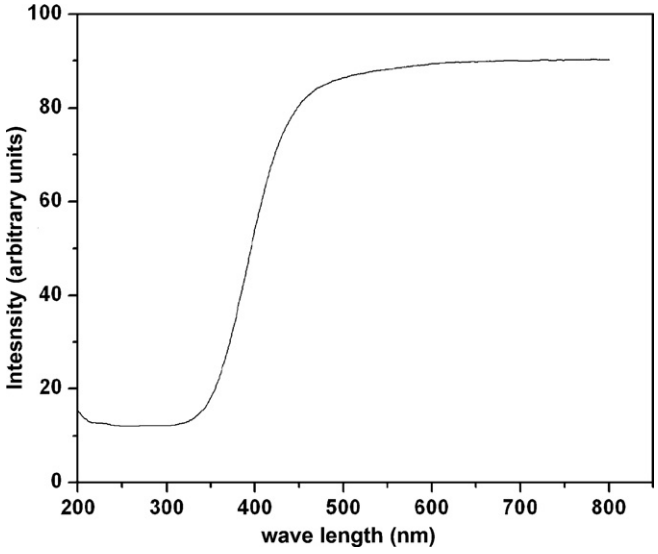

Fig. 6. Reflectance spectra $BaSnO_3$ obtained through combustion synthesis.

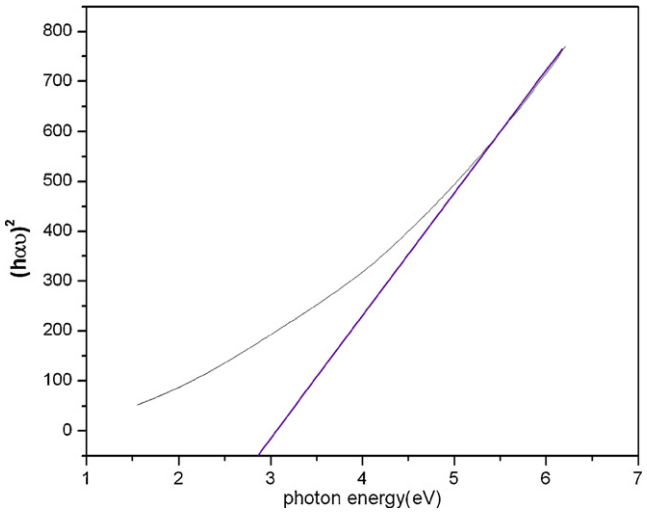

Fig. 7. Plot of $(h\nu\alpha)^2$ and $h\nu$ of $BaSnO_3$ nanoparticles.

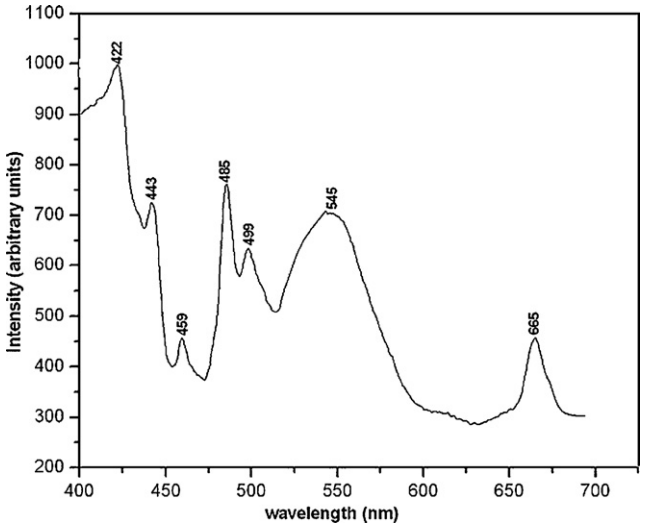

Fig. 8. Photoluminescent spectra of as-prepared $BaSnO_3$ nanopowder obtained through combustion synthesis.

the dimensions of materials are below a certain size. Also optical band gap of the samples is related to the crystalline nature. This establishes that the $BaSnO_3$ nanoparticles posses good crystalline structure. This is an added advantage that the pure sample showed decrease in band gap which is an indication of improved conductivity.

The photoluminescence spectra obtained at the excitation wavelength 350 nm of the sample is given in Fig. 8. The sample has intense emission in the visible region. The transition of the constituent elements of compounds causing emissions are identified on the basis of the data by Payling and Larkins [38]. The strong line at 665 nm is due to the transition $^3F^0{}_2$–$^3F_2$ of barium. The broad lines at 545 nm is due to the transitions $^3P^0{}_0$–$^3D_1$.The transitions at 499 and 485 nm corresponds to $^3P^2{}_0$–$^3D_3$ of barium and $^3P^0{}_1$–$^1D_2$ of tin respectively. The intense lines at 443 and 422 nm are the result of transitions of barium which are $^3P^0{}_0$–$^3D_1$ and $^3P^0{}_0$–$^3P_1$. Medium intense peak at 459 nm is due to the transition $^3P^0{}_1$–$^3D_1$ of tin.

The transmission electron microscopy (TEM) studies on the powder morphology of the as-prepared $BaSnO_3$ nanopowder obtained by the combustion synthesis shows that the nanoparticles are of submicron size 20–30 nm as shown in Fig. 9. The measured nanocrystalline grains are in the range from 20 to 30 nm with a majority particle size is 23 nm. Both agglomerates and nanocrystallites are of cuboidal shape. Individual crystallites in the agglomerates appear well bonded with few voids in between. About 85% of the particles in the powder had an average size of 20 nm and the remaining 15% of the particle had an average particle size of 30 nm. TEM shown as inset (a) in Fig. 9 clearly substantiates this. Further investigation of TEM images shows the presence of trace $BaCO_3$ [17]. The stick like $BaCO_3$ particles are shown in inset (b) of Fig. 9. Inset (c) of Fig. 9 shows a selected area electron diffraction (SAED) pattern recorded at an accelerating voltage of 200 kV, which corresponds to an electron wavelength of 2.508 pm, and at a camera length of 915 mm. The $BaSnO_3$ nanocrystals exhibit sparser rings in the electron diffraction pattern. This is indicative of the poly crystalline nature of the crystallites, but the spotty nature of the SAED pattern can be due to the fact that the finer crystallites having related orientations are agglomerated together resulting in a limited set of orientations. SAED pattern indexation shows that most of the diffracted spots information belongs to the $BaSnO_3$ crystalline structure. The ($h\,k\,l$) values corresponding to calculated d-spacings −1.466, 1.692 and 2.071 Å – are (2 2 0) (2 1 1) and (2 0 0) respectively and these are of $BaSnO_3$. A few diffuse spots can be seen

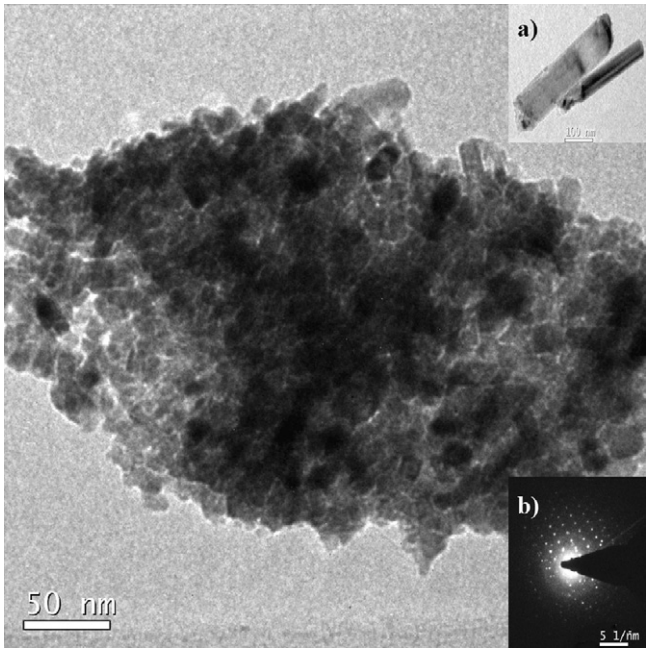

Fig. 9. The TEM micrographs of as-prepared $BaSnO_3$ nanopowder (a) HRTEM and (b) the corresponding electron diffraction pattern.

which point to the presence of trace $BaCO_3$ as observed in XRD and Raman Spectra of the as-prepared sample. The lattice image of the nanocrystalline particle showed very little distortion.

4. Conclusions

Nanocrystalline semiconducting $BaSnO_3$ was synthesized through a modified combustion process. The X-ray diffraction studies have shown that the nanopowder was single phase, crystalline, and has a cubic perovskite structure with a lattice constant $a = 4.115$ Å. The average particle size calculated from FWHM is ∼25 nm. The thermal stability of $BaSnO_3$ nanopowders has been confirmed using thermo gravimetric analysis (TGA) and differential thermal analysis (DTA). Fourier transform infrared spectroscopy (FTIR) and FT-Raman studies showed that samples heated up to 1200 °C posses an ideal cubic perovskite structure. The nanocyrstalline $BaSnO_3$ is found to be a photoluminescent material. The band gap determined from the UV–vis spectrum is 2.887 eV. TEM and SAED pattern confirms the nanocrystalline nature of the sample.

Acknowledgement

The authors acknowledge the University Grants Commission New Delhi for financial assistance.

References

[1] W. Zhang, J. Tang, J. Ye, J. Mater. Res. 22 (2007) 1859–1871.
[2] M.G. Smith, J.B. Goodenough, A. Manthiram, R.D. Taylor, W. Peng, C.W. Kimbal, J. Solid State Chem. 98 (1992) 181–186.
[3] T. Maekawa, K. Kurosaki, S. Yamanaka, J. Alloys Compd. 416 (2006) 214–217.
[4] R. Vivekanandan, T.R.N. Kutty, Ceram. Int. 14 (1988) 207–216.
[5] P.T. Moseley, D.E. Williams, B.C. Tofield, Sens. Actuators 14 (1988) 79–91.
[6] Y. Shimizu, M. Shimabukuro, H. Arai, T. Seiyama, J. Electrochem. Soc. 136 (1989) 1206–1210.
[7] U. Lumpe, J. Gerblinger, H. Meixner, Sens. Actuators B 24/25 (1995) 657–660.
[8] R. Ostrick, M. Fleischer, H. Meixner, J. Am. Ceram. Soc. 80 (1997) 2153–2156.
[9] H. Mizoguchi,.W. Eng, P.M. Woodward, Inorg. Chem. 43 (2004) 1667–1680.
[10] P.H. Borse, J.S. Lee, H.G. Kim, J. Appl. Phys. 100 (2006) 124915–124920.
[11] Y. Yuan, J. Lv, X. Jiang, Z. Li, T. Yu, Z. Zou, J. Ye, Appl. Phys. Lett. 91 (2007) 094107–094111.

[12] H. Mizoguchi, P.W. Woodward, C. Park, D.A. Keszler, J. Am. Chem. Soc. 126 (2004) 9796–9800.
[13] Z.G. Zhou, G. Zhao, M. Wei, Z.-T. Zhang, Ferroelectrics 101 (1990) 43–54.
[14] S. Upadhyay, Om Parkash, D. Kumar, Mater. Lett. 49 (2001) 251–255.
[15] M. Licheronb, G. Jouan, E. Husson, J. Euro. Ceram. Soc. 17 (1997) 1453–1457.
[16] T.R.N. Kutty, R. Vivekanadan, Mater. Res. Bull. 22 (1987) 1457–1465.
[17] Wensheng Lu, Helmut Schmidt, J. Euro. Ceram. Soc. 25 (2005) 919–925.
[18] C.P. Udawatte, M. Yoshimura, Mater. Lett. 47 (2001) 7–10.
[19] M. Leoni, M. Viviani, P. Nanni, V. Buscaglia, J. Mater. Sci. Lett. 15 (1996) 1302–1304.
[20] M.T. Buscaglia, M. Leoni, M. Viviani, V. Buscaglia, A. Martinelli, A. Testino, P. Nanni, J. Mater. Res. 18 (2003) 560–566.
[21] W. Lu, H. Schmidt, Ceram. Int. 34 (2008) 645–649.
[22] C.P. Udawatte, M. Kakihana, M. Yoshimura, Solid State Ionics 108 (1998) 23–30.
[23] W. Lu, H. Schmidt, J. Sol-Gel Sci. Technol. 42 (2007) 55–64.
[24] Y.J. Song, S. Kim, J. Ind. Eng. Chem. 7 (2001) 183–185.
[25] L. Jager, V. Lorenz, T. Muller, H.P. Abicht, M. Rossel, H. Gorls, Z. Anorg. Allg. Chem. 630 (2004) 189–195.
[26] M.D. Aguas, L. Morris, I.P. Parkin, J. Mater. Sci. 37 (2002) 375–379.
[27] A.M. Azad, L.L.W. Shyan, T.Y. Pang, C.H. Nee, Ceram. Int. 26 (2000) 685–692.
[28] J.J. Kingsley, K.C. Patil, Mater. Lett. 6 (1988) 427–432.
[29] P. Pramanik, Bull. Mater. Sci. 22 (1999) 335–339.
[30] S.D. Ross, Inorganic Infrared and Raman Spectra, second Ed., Mc Graw Hill Book Company, London, 1972.
[31] J. Cerda, J. Arbiol, Mater. Lett. 56 (2002) 131–136.
[32] W.G. Fateley, F.R. Dollish, N.T. McDevitt, F.F. Benthy, Infrared and Raman selection Rules for Molecules and Lattice vibrations: The Correlation Method, Third Ed., Wiley Interscience, New York, 1972.
[33] J.M. Worlock, S.P.S. Porto, Phys. Rev. Lett. 15 (1965) 697–699.
[34] L.B. Duan, G.H. Rao, Y.C. Wang, J. Yu, T. Wang, J. Appl. Phys. 123 (2008) 1–4.
[35] M.W. Charles, H. Nick Jr., E.S. Gregory, Physical Properties of Semiconductors, 49th Ed., Prentice-Hall, Englewood Cliffs, New Jersey, 1989.
[36] J. Cava, P. Gammel, B. Batlogg, J.J. Krajewski, W.F. Peck Jr., W.L. Rupp Jr., R. Felder, R.B. van Dover, Phys. Rev. B 42 (1990) 4815–4818.
[37] R. Koferstein, F. Yakuphanoglu, J. Alloys Compd. 506 (2010) 678–682.
[38] R. Payling, P. Larkins, Optical Emission Lines Of Elements, First Ed., John Wileyand sons, New York, June 2000.